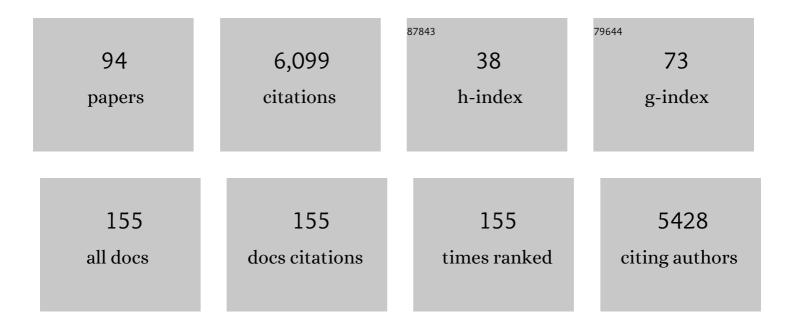
## Robert J Parker

List of Publications by Year in descending order

Source: https://exaly.com/author-pdf/2778315/publications.pdf Version: 2024-02-01



#	Article	IF	CITATIONS
1	The Global Methane Budget 2000–2017. Earth System Science Data, 2020, 12, 1561-1623.	3.7	1,199
2	UKESM1: Description and Evaluation of the U.K. Earth System Model. Journal of Advances in Modeling Earth Systems, 2019, 11, 4513-4558.	1.3	448
3	Estimating global and North American methane emissions with high spatial resolution using GOSAT satellite data. Atmospheric Chemistry and Physics, 2015, 15, 7049-7069.	1.9	225
4	Orbiting Carbon Observatory: Inverse method and prospective error analysis. Journal of Geophysical Research, 2008, 113, .	3.3	222
5	Global Characterization of CO2 Column Retrievals from Shortwave-Infrared Satellite Observations of the Orbiting Carbon Observatory-2 Mission. Remote Sensing, 2011, 3, 270-304.	1.8	215
6	Methane observations from the Greenhouse Gases Observing SATellite: Comparison to groundâ€based TCCON data and model calculations. Geophysical Research Letters, 2011, 38, .	1.5	211
7	Atmospheric carbon dioxide retrieved from the Greenhouse gases Observing SATellite (GOSAT): Comparison with groundâ€based TCCON observations and GEOSâ€Chem model calculations. Journal of Geophysical Research, 2012, 117, .	3.3	139
8	Toward robust and consistent regional CO <sub>2</sub> flux estimates from in situ and spaceborne measurements of atmospheric CO <sub>2</sub> . Geophysical Research Letters, 2014, 41, 1065-1070.	1.5	126
9	Inverse modelling of CH <sub>4</sub> emissions for 2010–2011 using different satellite retrieval products from GOSAT and SCIAMACHY. Atmospheric Chemistry and Physics, 2015, 15, 113-133.	1.9	126
10	The Greenhouse Gas Climate Change Initiative (GHG-CCI): Comparison and quality assessment of near-surface-sensitive satellite-derived CO2 and CH4 global data sets. Remote Sensing of Environment, 2015, 162, 344-362.	4.6	112
11	Global distribution of methane emissions, emission trends, and OH concentrations and trends inferred from an inversion of GOSAT satellite data for 2010–2015. Atmospheric Chemistry and Physics, 2019, 19, 7859-7881.	1.9	111
12	Global atmospheric carbon monoxide budget 2000–2017 inferred from multi-species atmospheric inversions. Earth System Science Data, 2019, 11, 1411-1436.	3.7	96
13	Estimating regional methane surface fluxes: the relative importance of surface and GOSAT mole fraction measurements. Atmospheric Chemistry and Physics, 2013, 13, 5697-5713.	1.9	94
14	Spatially resolving methane emissions in California: constraints from the CalNex aircraft campaign and from present (GOSAT, TES) and future (TROPOMI, geostationary) satellite observations. Atmospheric Chemistry and Physics, 2014, 14, 8173-8184.	1.9	93
15	On the consistency between global and regional methane emissions inferred from SCIAMACHY, TANSO-FTS, IASI and surface measurements. Atmospheric Chemistry and Physics, 2014, 14, 577-592.	1.9	91
16	Satellite-inferred European carbon sink larger than expected. Atmospheric Chemistry and Physics, 2014, 14, 13739-13753.	1.9	83
17	Estimates of European uptake of CO <sub>2</sub> inferred from GOSAT X <sub>CO<sub>2</sub></sub> retrievals: sensitivity to measurement bias inside and outside Europe. Atmospheric Chemistry and Physics, 2016, 16, 1289-1302.	1.9	77
18	Advancing Scientific Understanding of the Global Methane Budget in Support of the Paris Agreement. Global Biogeochemical Cycles, 2019, 33, 1475-1512.	1.9	73

**ROBERT J PARKER** 

#	Article	IF	CITATIONS
19	The Greenhouse Gas Climate Change Initiative (GHG-CCI): comparative validation of GHG-CCI SCIAMACHY/ENVISAT and TANSO-FTS/GOSAT CO <sub>2</sub> and CH <sub>4</sub> retrieval algorithm products with measurements from the TCCON. Atmospheric Measurement Techniques, 2014, 7, 1723-1744.	1.2	70
20	Attribution of the accelerating increase in atmospheric methane during 2010–2018 by inverse analysis of GOSAT observations. Atmospheric Chemistry and Physics, 2021, 21, 3643-3666.	1.9	68
21	Atmospheric observations show accurate reporting and little growth in India's methane emissions. Nature Communications, 2017, 8, 836.	5.8	67
22	Assessing 5 years of GOSAT Proxy XCH <sub>4</sub> data and associated uncertainties. Atmospheric Measurement Techniques, 2015, 8, 4785-4801.	1.2	64
23	Does GOSAT capture the true seasonal cycle of carbon dioxide?. Atmospheric Chemistry and Physics, 2015, 15, 13023-13040.	1.9	63
24	Satellite-derived methane hotspot emission estimates using a fast data-driven method. Atmospheric Chemistry and Physics, 2017, 17, 5751-5774.	1.9	63
25	A joint effort to deliver satellite retrieved atmospheric CO <sub>2</sub> concentrations for surface flux inversions: the ensemble median algorithm EMMA. Atmospheric Chemistry and Physics, 2013, 13, 1771-1780.	1.9	62
26	Variability of fire carbon emissions in equatorial Asia and its nonlinear sensitivity to El Niño. Geophysical Research Letters, 2016, 43, 10,472.	1.5	60
27	An increase in methane emissions from tropical Africa between 2010 and 2016 inferred from satellite data. Atmospheric Chemistry and Physics, 2019, 19, 14721-14740.	1.9	58
28	Mixed deposits of complex magmatic and phreatomagmatic volcanism: an example from Crater Hill, Auckland, New Zealand. Bulletin of Volcanology, 1996, 58, 59-66.	1.1	55
29	Evaluating year-to-year anomalies in tropical wetland methane emissions using satellite CH4 observations. Remote Sensing of Environment, 2018, 211, 261-275.	4.6	55
30	Global methane budget and trend, 2010–2017: complementarity of inverse analyses using in situ (GLOBALVIEWplus CH <sub>4</sub> ObsPack) and satellite (GOSAT) observations. Atmospheric Chemistry and Physics, 2021, 21, 4637-4657.	1.9	55
31	Global distribution of methane emissions: a comparative inverse analysis of observations from the TROPOMI and GOSAT satellite instruments. Atmospheric Chemistry and Physics, 2021, 21, 14159-14175.	1.9	54
32	A decade of GOSAT Proxy satellite CH <sub>4</sub> observations. Earth System Science Data, 2020, 12, 3383-3412.	3.7	53
33	Clobal satellite observations of column-averaged carbon dioxide and methane: The GHG-CCI XCO2 and XCH4 CRDP3 data set. Remote Sensing of Environment, 2017, 203, 276-295.	4.6	52
34	Consistent regional fluxes of CH <sub>4</sub> and CO <sub>2</sub> inferred from GOSAT proxy XCH <sub>4</sub> â€`:â€`XCO <sub>2</sub> retrieva 2010–2014. Atmospheric Chemistry and Physics, 2017, 17, 4781-4797.	als,	52
35	Attribution of recent increases in atmospheric methane through 3-D inverse modelling. Atmospheric Chemistry and Physics, 2018, 18, 18149-18168.	1.9	51
36	Atmospheric CH <sub>4</sub> and CO <sub>2</sub> enhancements and biomass burning emission ratios derived from satellite observations of the 2015 Indonesian fire plumes. Atmospheric Chemistry and Physics, 2016, 16, 10111-10131.	1.9	49

Robert J Parker

#	Article	IF	CITATIONS
37	Effects of atmospheric light scattering on spectroscopic observations of greenhouse gases from space. Part 2: Algorithm intercomparison in the GOSAT data processing for CO <sub>2</sub> retrievals over TCCON sites. Journal of Geophysical Research D: Atmospheres, 2013, 118, 1493-1512.	1.2	46
38	HDO/H <sub>2</sub> O ratio retrievals from GOSAT. Atmospheric Measurement Techniques, 2013, 6, 599-612.	1.2	45
39	Influence of differences in current GOSAT <i><b>X</b></i> <b><sub>CO</sub><sub>2</sub></b> retrievals on surface flux estimation. Geophysical Research Letters, 2014, 41, 2598-2605.	1.5	45
40	2010–2015 North American methane emissions, sectoral contributions, and trends: a high-resolution inversion of GOSAT observations of atmospheric methane. Atmospheric Chemistry and Physics, 2021, 21, 4339-4356.	1.9	45
41	Effects of atmospheric light scattering on spectroscopic observations of greenhouse gases from space: Validation of PPDFâ€based CO <sub>2</sub> retrievals from GOSAT. Journal of Geophysical Research, 2012, 117, .	3.3	42
42	Role of regional wetland emissions in atmospheric methane variability. Geophysical Research Letters, 2016, 43, 11,433.	1.5	37
43	Tropical land carbon cycle responses to 2015/16 El Niño as recorded by atmospheric greenhouse gas and remote sensing data. Philosophical Transactions of the Royal Society B: Biological Sciences, 2018, 373, 20170302.	1.8	37
44	First satellite measurements of carbon dioxide and methane emission ratios in wildfire plumes. Geophysical Research Letters, 2013, 40, 4098-4102.	1.5	36
45	Estimating regional fluxes of CO <sub>2</sub> and CH <sub>4</sub> using space-borne observations of XCH <sub>4</sub> : XCO <sub>2</sub> . Atmospheric Chemistry and Physics. 2014. 14. 12883-12895.	1.9	35
46	2010–2016 methane trends over Canada, the United States, and Mexico observed by the GOSAT satellite: contributions from different source sectors. Atmospheric Chemistry and Physics, 2018, 18, 12257-12267.	1.9	35
47	Evaluation of errors from neglecting polarization in the forward modeling of O2 A band measurements from space, with relevance to CO2 column retrieval from polarization-sensitive instruments. Journal of Quantitative Spectroscopy and Radiative Transfer, 2007, 103, 245-259.	1.1	34
48	Quantifying lower tropospheric methane concentrations using GOSAT near-IR and TES thermal IR measurements. Atmospheric Measurement Techniques, 2015, 8, 3433-3445.	1.2	34
49	Observations of an atmospheric chemical equator and its implications for the tropical warm pool region. Journal of Geophysical Research, 2008, 113, .	3.3	31
50	Natural and anthropogenic methane fluxes in Eurasia: a mesoscale quantification by generalized atmospheric inversion. Biogeosciences, 2015, 12, 5393-5414.	1.3	31
51	Tropical methane emissions explain large fraction of recent changes in global atmospheric methane growth rate. Nature Communications, 2022, 13, 1378.	5.8	31
52	A measurement-based verification framework for UK greenhouse gas emissions: an overview of the Greenhouse gAs Uk and Global Emissions (GAUGE) project. Atmospheric Chemistry and Physics, 2018, 18, 11753-11777.	1.9	29
53	Rain-fed pulses of methane from East Africa during 2018–2019 contributed to atmospheric growth rate. Environmental Research Letters, 2021, 16, 024021.	2.2	28
54	Can a regional-scale reduction of atmospheric CO <sub>2</sub> during the COVID-19 pandemic be detected from space? A case study for East China using satellite XCO <sub>2</sub> retrievals. Atmospheric Measurement Techniques, 2021, 14, 2141-2166.	1.2	28

**ROBERT J PARKER** 

#	Article	IF	CITATIONS
55	Computation and analysis of atmospheric carbon dioxide annual mean growth rates from satellite observations during 2003–2016. Atmospheric Chemistry and Physics, 2018, 18, 17355-17370.	1.9	27
56	Characterizing model errors in chemical transport modeling of methane: impact of model resolution in versions v9-02 of GEOS-Chem and v35j of its adjoint model. Geoscientific Model Development, 2020, 13, 3839-3862.	1.3	27
57	Toward High Precision XCO <sub>2</sub> Retrievals From TanSat Observations: Retrieval Improvement and Validation Against TCCON Measurements. Journal of Geophysical Research D: Atmospheres, 2020, 125, e2020JD032794.	1.2	25
58	Methane emissions in the United States, Canada, and Mexico: evaluation of national methane emission inventories and 2010–2017 sectoral trends by inverse analysis of in situ (GLOBALVIEWplus) Tj ETQq0 0 0 rg	3T /Qverloc 1.9	k 10 Tf 50 62
	Atmospheric Chemistry and Physics, 2022, 22, 395-418.		
59	Accelerating methane growth rate from 2010 to 2017: leading contributions from the tropics and East Asia. Atmospheric Chemistry and Physics, 2021, 21, 12631-12647.	1.9	23
60	Intercomparison of integrated IASI and AATSR calibrated radiances at 11 and 12 $\hat{I}$ /4m. Atmospheric Chemistry and Physics, 2009, 9, 6677-6683.	1.9	22
61	Impact of Aerosol Property on the Accuracy of a CO2 Retrieval Algorithm from Satellite Remote Sensing, 2016, 8, 322.	1.8	22
62	Ensemble-based satellite-derived carbon dioxide and methane column-averaged dry-air mole fraction data sets (2003–2018) for carbon and climate applications. Atmospheric Measurement Techniques, 2020, 13, 789-819.	1.2	22
63	The added value of satellite observations of methane forunderstanding the contemporary methane budget. Philosophical Transactions Series A, Mathematical, Physical, and Engineering Sciences, 2021, 379, 20210106.	1.6	21
64	Sustained methane emissions from China after 2012 despite declining coal production and rice-cultivated area. Environmental Research Letters, 2021, 16, 104018.	2.2	19
65	A New TanSat XCO2 Global Product towards Climate Studies. Advances in Atmospheric Sciences, 2021, 38, 8-11.	1.9	19
66	CH <sub>4</sub> concentrations over the Amazon from GOSAT consistent with in situ vertical profile data. Journal of Geophysical Research D: Atmospheres, 2016, 121, 11,006.	1.2	18
67	Global height-resolved methane retrievals from the Infrared Atmospheric Sounding Interferometer (IASI) on MetOp. Atmospheric Measurement Techniques, 2017, 10, 4135-4164.	1.2	18
68	A new space-borne perspective of crop productivity variations over the US Corn Belt. Agricultural and Forest Meteorology, 2020, 281, 107826.	1.9	17
69	Monitoring Greenhouse Gases from Space. Remote Sensing, 2021, 13, 2700.	1.8	17
70	Quantifying sources of Brazil's CH <sub>4</sub> emissions between 2010 and 2018 from satellite data. Atmospheric Chemistry and Physics, 2020, 20, 13041-13067.	1.9	17
71	Retrieval of from simulated Orbiting Carbon Observatory measurements using the fast linearized Râ€2OS radiative transfer model. Journal of Geophysical Research, 2008, 113, .	3.3	16
72	Copernicus Climate Change Service (C3S) Global Satellite Observations of Atmospheric Carbon Dioxide and Methane. Advances in Astronautics Science and Technology, 2018, 1, 57-60.	0.5	16

Robert J Parker

#	Article	IF	CITATIONS
73	Exploring constraints on a wetland methane emission ensemble (WetCHARTs) using GOSAT observations. Biogeosciences, 2020, 17, 5669-5691.	1.3	16
74	Acetylene C <sub>2</sub> H <sub> 2</sub> retrievals from MIPAS data and regions of enhanced upper tropospheric concentrations in August 2003. Atmospheric Chemistry and Physics, 2011, 11, 10243-10257.	1.9	14
75	Characterizing model errors in chemical transport modeling of methane: using GOSAT XCH <sub>4</sub> data with weak-constraint four-dimensional variational data assimilation. Atmospheric Chemistry and Physics, 2021, 21, 9545-9572.	1.9	14
76	Large Methane Emission Fluxes Observed From Tropical Wetlands in Zambia. Global Biogeochemical Cycles, 2022, 36, .	1.9	14
77	Estimates of North African Methane Emissions from 2010 to 2017 Using GOSAT Observations. Environmental Science and Technology Letters, 2021, 8, 626-632.	3.9	13
78	Large and increasing methane emissions from eastern Amazonia derived from satellite data, 2010–2018. Atmospheric Chemistry and Physics, 2021, 21, 10643-10669.	1.9	13
79	The Physical Climate at Global Warming Thresholds as Seen in the U.K. Earth System Model. Journal of Climate, 2022, 35, 29-48.	1.2	12
80	Study of the footprints of short-term variation in XCO <sub>2</sub> observed by TCCON sites using NIES and FLEXPART atmospheric transport models. Atmospheric Chemistry and Physics, 2017, 17, 143-157.	1.9	10
81	Observing Water Vapour in the Planetary Boundary Layer from the Short-Wave Infrared. Remote Sensing, 2018, 10, 1469.	1.8	10
82	Retrieval of greenhouse gases from GOSAT and GOSAT-2 using the FOCAL algorithm. Atmospheric Measurement Techniques, 2022, 15, 3401-3437.	1.2	10
83	Description and Evaluation of an Emissionâ€Driven and Fully Coupled Methane Cycle in UKESM1. Journal of Advances in Modeling Earth Systems, 2022, 14, .	1.3	9
84	Retrieving XCO2 from GOSAT FTS over East Asia Using Simultaneous Aerosol Information from CAI. Remote Sensing, 2016, 8, 994.	1.8	8
85	Seasonal and Inter-annual Variation of Evapotranspiration in Amazonia Based on Precipitation, River Discharge and Gravity Anomaly Data. Frontiers in Earth Science, 2019, 7, .	0.8	8
86	Large Methane Emissions From the Pantanal During Rising Water‣evels Revealed by Regularly Measured Lower Troposphere CH <sub>4</sub> Profiles. Global Biogeochemical Cycles, 2021, 35, e2021GB006964.	1.9	8
87	Atmospheric observations consistent with reported decline in the UK's methane emissions (2013–2020). Atmospheric Chemistry and Physics, 2021, 21, 16257-16276.	1.9	8
88	GreenHouse gas Observations of the Stratosphere and Troposphere (GHOST): an airborne shortwave-infrared spectrometer for remote sensing of greenhouse gases. Atmospheric Measurement Techniques, 2018, 11, 5199-5222.	1.2	6
89	Earth system music: music generated from the United Kingdom Earth System Model (UKESM1). Geoscience Communication, 2020, 3, 263-278.	0.5	4
90	An integrated analysis of contemporary methane emissions and concentration trends over China using in situ and satellite observations and model simulations. Atmospheric Chemistry and Physics, 2022, 22, 1229-1249.	1.9	3

#	Article	IF	CITATIONS
91	The greenhouse gas project of ESA's climate change initiative (GHG-CCI): overview, achievements and future plans. International Archives of the Photogrammetry, Remote Sensing and Spatial Information Sciences - ISPRS Archives, 0, XL-7/W3, 165-172.	0.2	1
92	The Significance of Fast Radiative Transfer for Hyperspectral SWIR XCO2 Retrievals. Atmosphere, 2020, 11, 1219.	1.0	1
93	Methane Growth Rate Estimation and Its Causes in Western Canada Using Satellite Observations. Journal of Geophysical Research D: Atmospheres, 2021, 126, e2020JD033948.	1.2	1
94	Comparative multifractal analysis of methane gas concentration time series in India and regions within India. Proceedings of the Indian National Science Academy, 0, , .	0.5	0